REPRODUCTION
RESEARCH

Dynamics of constitutive heterochromatin: two contrasted kinetics of genome restructuring in early cloned bovine embryos

Andrey Pichugin[1,2], Daniel Le Bourhis[1,2,3], Pierre Adenot[1,2], Gaëtan Lehmann[1,2], Christophe Audouard[1,2], Jean-Paul Renard[1,2], Xavier Vignon[1,2] and Nathalie Beaujean[1,2]

[1]*INRA and* [2]*ENVA, UMR 1198 Biologie du développement et reproduction, F-78350 Jouy en Josas, France and* [3]*UNCEIA Département R&D, 13, rue Jouet, 94703 Maison-Alfort Cedex, France*

Correspondence should be addressed to X Vignon; Email: xavier.vignon@jouy.inra.fr
N Beaujean; Email: nathalie.beaujean@jouy.inra.fr

Abstract

Efficient reprograming of the donor cell genome in nuclear transfer (NT) embryos is linked to the ability of the embryos to sustain full-term development. As the nuclear architecture has recently emerged as a key factor in the regulation of gene expression, we questioned whether early bovine embryos obtained from transfer of cultured fibroblasts into enucleated oocytes would adopt an embryo-like nuclear organization. We studied the dynamics of constitutive heterochromatin in the stages prior to embryonic genome activation by distribution analysis of heterochromatin protein CBX1 (HP1), centromeric proteins CENPA and CENPB, and histone H3 three-methylated at lysine 9. Then we applied descriptive, quantitative, and co-localization analyses. A dramatic reorganization of heterochromatic blocks of somatic donor cells was first observed in the late one-cell stage NT embryos. Then at two- and four-cell stages, we found two types of NT embryos: one displaying noncondensed heterochromatin patches similar to IVF embryos, whereas the second type displayed condensed heterochromatin blocks, normally observed in IVF embryos only after the eight-cell stage. These analyses discriminate for the first time two contrasted types of nuclear organization in NT embryos, which may correspond to different functional states of the nuclei. The relationship with the somatic nucleus reprograming efficiency is discussed.

Reproduction (2010) **139** 129–137

Introduction

Although the transfer of differentiated nuclei has successfully led to full-term development of viable and fertile offspring in several mammalian species, the reconstructed embryos still have low rates of development. It is now believed that epigenetic changes, such as histones post-translational modifications and DNA methylation, could affect gene expression in nuclear transfer (NT) embryos and thereby influence NT efficiency (Fulka *et al*. 2008, Loi *et al*. 2008). Such changes are known to induce chromatin remodelling and thereby nuclear higher order structures reorganization (Schneider & Grosschedl 2007). Therefore, understanding how the donor cell genome is reorganized upon NT could be helpful to improve animal cloning procedures.

In somatic cell nuclei, pericentric regions from several chromosomes have been shown to form blocks of constitutive heterochromatin called chromocenters (Cerda *et al*. 1999). These chromocenters are characterized by specific epigenetic modifications such as highly methylated DNA and trimethylation at lysine 9 of histone H3 (H3K9me3; Goll & Bestor 2002, Lachner *et al*. 2003). Then methylated H3K9 provides a binding site for proteins with silencing properties such as heterochromatin protein 1 (HP1 or CBX1). This protein is known to induce transcriptional repression and propagation of heterochromatin at chromocenters (Cheutin *et al*. 2003, Hayakawa *et al*. 2003). In somatic cells, chromocenters form, at the cytological level, globular blocks of heterochromatin associated with the centromeric regions that contain the centromeric proteins CENP (Prusov & Zatzepina 2002). However, the structure and distribution of chromocenters is cell type specific and may vary among mammalian species, as well as the associated epigenetic marks (Solovei *et al*. 2004, Brero *et al*. 2005, Mayer *et al*. 2005, Wiblin *et al*. 2005).

In mammalian embryos, the first cellular cycles are characterized by modifications of several epigenetic marks, and specific nuclear reorganization is observed during the preimplantation development. In mouse, active demethylation of the paternal genome has been observed just after fertilization, followed by passive demethylation during the next stages, and *de novo* methylation at the peri-implantation period (Mayer *et al*. 2000, Santos *et al*. 2002). It was also previously shown that both parental genomes display a peculiar

ISSN 1470–1626 (paper) 1741–7899 (online)
DOI: 10.1530/REP-08-0435
Online version via www.reproduction-online.org

distribution of pericentric heterochromatin and centromeres, organized around nucleolar precursor bodies (Martin *et al*. 2006*b*, Merico *et al*. 2007, Probst *et al*. 2007). Chromocenter genesis is then achieved by the end of the two-cell stage. In cows, the genome undergoes a delayed demethylation (Santos *et al*. 2002), and homogenous CBX1 labeling with random distribution of centromeres is observed during the three first cell cycles, and chromocenters are then progressively established (Martin *et al*. 2006*a*). Remarkably, these dynamics of epigenetic marks and reorganization of nuclear architecture appear tightly connected to the functional state of the genome. Establishment of chromocenters in mouse and bovine embryos, for example, correlates with the transcriptional activation of the embryonic genome (EGA; Latham 1999, Martin *et al*. 2006*a*).

The embryos derived from somatic cell NT (SCNT) are supposed to undergo reprograming in order to sustain full-term development. This includes epigenetic marks and nucleolar reprograming (Maddox-Hyttel *et al*. 2005, Fulka *et al*. 2008, Loi *et al*. 2008). However, the reprograming of the global nuclear organization and of higher order chromatin structures has been less investigated. In mouse, dramatic reorganization of donor cell nuclei has been described in few studies. Chromocenters, for example, display extensive disassembling during the first cell cycle after NT; and most chromocenters then reappear at the two-cell stage, concurrently with EGA (Martin *et al*. 2006*a*, 2006*b*, Merico *et al*. 2007). However, due to the short delay between one-cell stage and EGA (two-cell stage) in mouse, studying nuclear reprograming in this species is difficult. Here, we investigated bovine embryos that provide the opportunity to distinguish nuclear reorganizations occurring just after NT (one-cell stage) and at EGA (eight-cell stage). We focused on pericentric heterochromatin distribution and chromocenter genesis. We therefore performed immunostaining for CBX1, H3K9me3, and CENPA and CENPB in bovine embryos after NT or IVF. We applied descriptive, quantitative, and co-localization analyses. Our results show that two types of embryos with contrasted nuclear organization can be distinguished among the early NT bovine embryos from the two-cell stage onwards.

Results

Our routine procedures for IVF and somatic NT give high rates of development *in vitro*. In experiments performed concomitantly to the present study, we indeed recorded more than 51% of blastocysts derived from the embryos reconstructed by somatic NT or fertilized *in vitro* (Table 1). The two techniques therefore appear equally efficient in our hands.

Table 1 Developmental rates of somatic cell nuclear transfer (SCNT) embryos and IVF embryos.

	Embryos fused (SCNT) **or fertilized** (IVF)	**Cleaved embryos, two-cell stage**	**Morula** (day 5)	**Blastocyst** (day 7)
SCNT	197	159 (80.7%)	112 (56.8%)	102 (51.7%)
IVF	778	672 (86.4%)	423 (54.4%)	398 (51.2%)

Detection of CBX1 and CENP in IVF versus NT embryos

As shown in Fig. 1, bovine fibroblasts nuclei present the well-known chromocenters, i.e. globular CBX1 blocks with associated CENP dots. It should be mentioned here that the fibroblasts donor population, at confluence before NT, was quite homogeneous and that all cells exhibited a similar pattern (not shown). In embryonic cells of one- to four-cell stage IVF embryos, nuclear distribution of these proteins was different. Three types of CBX1 distribution could indeed be identified based on morphological criteria. First, the spread pattern characterized by uniform CBX1 staining (Fig. 1(i)) with few CBX1-condensed patches (1–4) and with random distribution of CENP dots. Second, the fibrous pattern

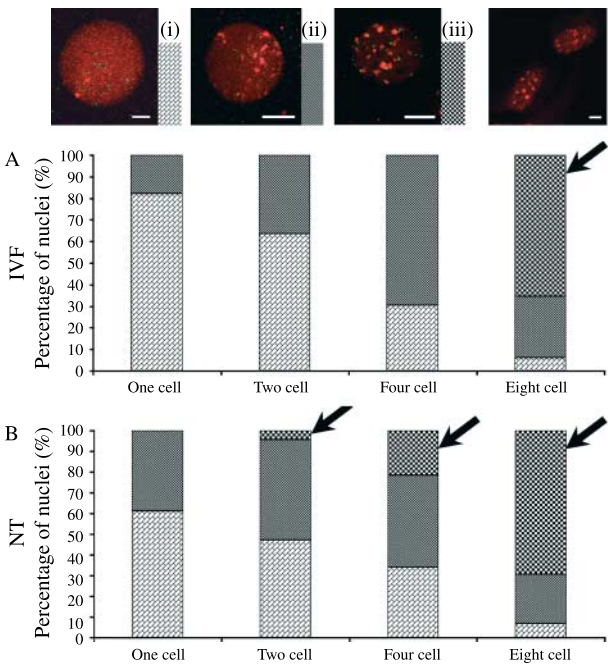

Figure 1 Upper panel: simultaneous CBX1 (red) and CENPA and CENPB (green) immunostaining revealed three patterns of heterochromatin identified on morphological criteria as spread ((i) two-cell IVF), fibrous ((ii) four-cell IVF), and globular ((iii) eight-cell IVF). Cultured primary bovine fibroblasts (right) exhibited the globular pattern. Scale bars: 5 μm. Lower panel: frequency of nuclei with each of three patterns at the different developmental stages was investigated in IVF (A) and NT (B) embryos. Burst of heterochromatin condensation was observed at eight-cell stage in IVF embryos (A), whereas increase in heterochromatin condensation began from two-cell stage in NT embryos (B). Arrows indicate fraction of nuclei with globular pattern.

characterized by small CBX1 blocks displaying various levels of heterochromatin condensation and that distributed independently of CENP dots (Fig. 1(ii)). These two patterns are embryo specific, but globular blocks of CBX1 associated with centromeres could also be observed (Fig. 1(iii)).

According to these patterns, we classified the nuclei of 104 IVF embryos ($n=382$ nuclei; Fig. 1A). At the one-cell stage, both male and female pronuclei displayed predominantly the spread pattern (82%, $n=16$), whereas the fibrous pattern was prevalent at the four-cell stage (70%, $n=116$). Both patterns then had a tendency to disappear at the eight-cell stage: only 6% of the nuclei displayed the spread pattern and 28% the fibrous pattern ($n=176$). The majority of nuclei at that stage displayed chromocenter-like structures (66%). Interestingly, only eight-cell stage embryos had such pattern suggesting a drastic heterochromatin compaction between the four- and eight-cell stages leading to chromocenter formation.

In comparison, the dynamics of these patterns during early embryonic development was clearly different in NT embryos (141 embryos; $n=459$ nuclei; Fig. 1B). The spread pattern was less predominant during the one-cell stage (62%, $n=49$), although it followed the same tendency to decrease from the one- to the eight-cell stage. In fact, in comparison to IVF embryos, the percentage of nuclei with a fibrous pattern was higher in one- (38%, $n=49$ vs 18%, $n=16$) and two-cell stage NT embryos (49%, $n=70$ nuclei versus 36%, $n=74$), but much lower at the four-cell stage (40%, $n=120$). Interestingly, globular CBX1 blocks associated with CENP could already be observed at the two- and four-cell stages (4%, $n=70$ and 22%, $n=120$ nuclei respectively). Moreover, these nuclear structures are similar to the chromocenters observed in eight-cell stage NT embryos (69%, $n=220$) suggesting an earlier compaction of heterochromatin in NT versus IVF embryos.

Finally, it should be noted than in both IVF and NT embryos, all nuclei within one embryo displayed a similar pattern of CBX1 distribution.

Quantitative analysis of heterochromatin condensation in IVF and NT embryos

In order to objectively characterize the dynamics of heterochromatin condensation, we applied quantitative analysis of CBX1 distribution in embryonic nuclei with preserved three-dimensional structure. Imaging was hence performed on a confocal microscope producing high-quality images that could be processed with computational approaches. With this analysis, CBX1 pattern is characterized by granules of different volume ranging from 0.06 to 10 μm^3 (Fig. 2). The number and the

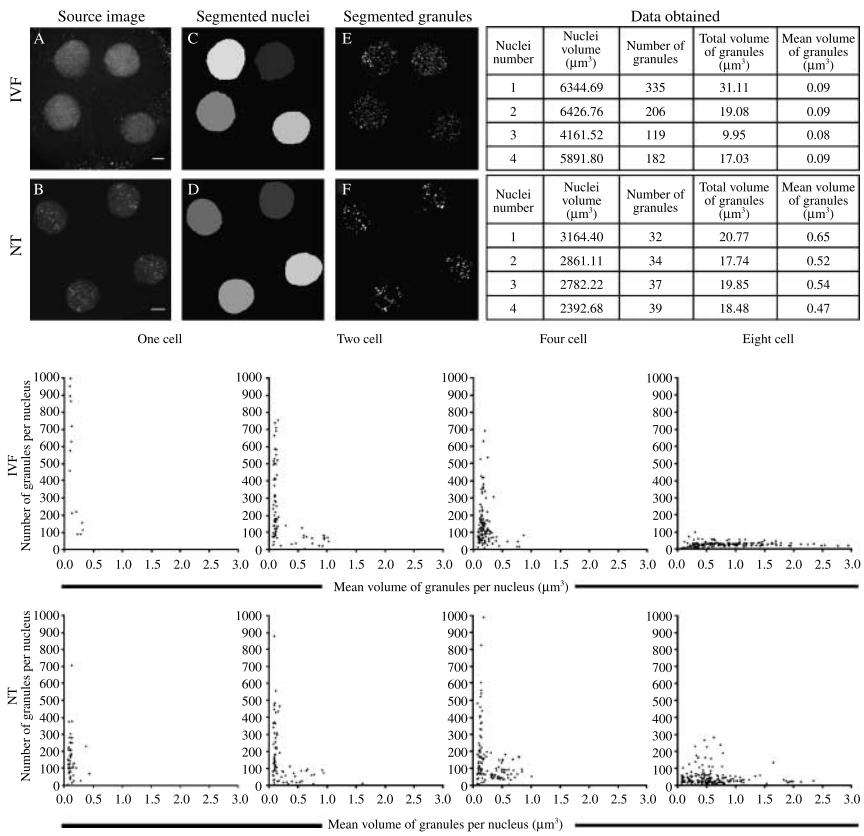

Nuclei number	Nuclei volume (μm^3)	Number of granules	Total volume of granules (μm^3)	Mean volume of granules (μm^3)
1	6344.69	335	31.11	0.09
2	6426.76	206	19.08	0.09
3	4161.52	119	9.95	0.08
4	5891.80	182	17.03	0.09

Nuclei number	Nuclei volume (μm^3)	Number of granules	Total volume of granules (μm^3)	Mean volume of granules (μm^3)
1	3164.40	32	20.77	0.65
2	2861.11	34	17.74	0.52
3	2782.22	37	19.85	0.54
4	2392.68	39	18.48	0.47

Figure 2 Automatic detection of nuclei and CBX1 granules, and their quantitative parameters. Upper panel: confocal Z-stack images from the three dimensionally preserved embryonic nuclei stained by anti-CBX1 antibodies (A and B) have been segmented by software (see Materials and Methods) for automatic detection of nuclear territory (C and D) and CBX1 granules (E and F). Gray-scale selection of nuclei in the images (C) and (D) corresponds to an individual number of nuclei in vertical order. Scale bars: 5 μm. Quantitative data obtained after software analysis of the example (four-cell stage embryos) are shown in the tables (IVF upper table, NT lower table). Lower panel: number and mean size of CBX1 granules in IVF and NT embryos at one- to eight-cell stages. Low mean size of granules (0.06–0.29 μm^3) was predominant in one- to four-cell stages. The mean size of granules is increased (0.3–3.0 μm^3) in nuclei of eight-cell IVF and in nuclei of two-, four-, and eight-cell stage NT embryos.

volume of these granules were given for each nucleus (Fig. 2). With this approach, we analyzed the same embryonic nuclei as above, according to their developmental stage.

Results (Fig. 2) show that nuclei with numerous granules (up to 1000) were prevalent in the one- to four-cell stages and that eight-cell stage nuclei display much less granules (<100). As expected, the chromocenters were easily detected as large granules (>0.3 μm^3) at that stage. We therefore used that parameter to distinguish noncondensed versus condensed heterochromatin: nuclei were classified according to the number of small versus large CBX1 granules ranging from 0.06 to 0.29 μm^3 (2–9 voxels) and from 0.3 to 2.5 μm^3 (10–85 voxels) respectively. The results, in accordance with our morphological analysis, demonstrate that the percentage of nuclei with large granules drastically increased between the four-cell stage (12%, $n=116$) and the eight-cell stage (86%, $n=176$) in IVF embryos (Fig. 3).

Two types of nuclei, with large or small granules, were also identified in early NT embryos (Figs 2 and 3). In comparison to our morphological analysis, a significantly higher percentage of nuclei with large granules was observed in two- (25%, $n=70$ vs 11%, $n=74$; $P<0.05$) and four-cell (42%, $n=120$ vs 12%, $n=116$; $P<0.001$) stage embryos, but reached the same level in eight-cell NT embryos as in IVF ones (86%, $n=220$). These quantitative data underline the presence of condensed heterochromatin at very early stages in NT embryos and confirm the precocious heterochromatin condensation in NT embryos versus IVF embryos.

Co-localization analysis of CBX1 and H3K9me3 labeling

To further investigate constitutive heterochromatin dynamics in bovine embryos, we then performed indirect immunofluorescent detection of CBX1 and H3K9me3. H3K9me3 is a modified histone specifically present in blocks of constitutive heterochromatin that co-localizes with CBX1 in chromocenters of cultured bovine fibroblasts. However, this was not the case in early stage embryos.

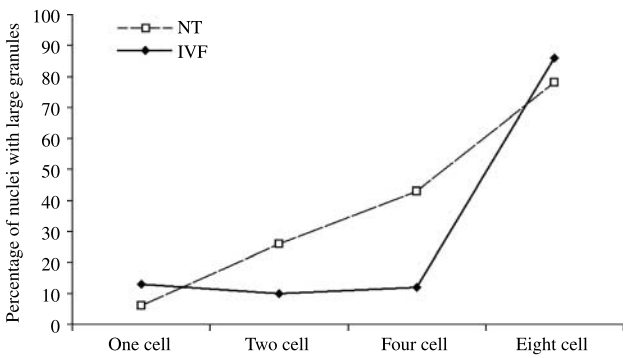

Figure 3 Percentage of nuclei with large CBX1 granules (more than 0.3 μm^3) in one- to eight-cell stage IVF and NT embryos.

At the one-cell stage, parental pronuclei of IVF embryos displayed opposite staining. Whereas the H3K9me3 was organized in patches gathered on one side in one pronucleus, the other one did not have this mark or displayed a very faint staining ($n=16$, Fig. 4A). Based on previous observations and on size differences between the two pronuclei as in other species (Park *et al.* 2007), we hypothesize that the male pronucleus is the one more weakly stained for H3K9me3. Computational co-localization analysis also showed that H3K9me3 and CBX1 labeling are not correlated at that stage (Fig. 5A).

In two- and four-cell stage IVF embryos, all nuclei analyzed ($n=64$ and $n=108$ respectively) often displayed a polarized distribution of H3K9me3 labeling (Fig. 4A). Some nuclei – that always corresponded to nuclei with a fibrous CBX1 pattern – had locally condensed H3K9me3 foci (12 and 11% respectively). Nevertheless, there was still no strict co-localization between CBX1 and H3K9me3 distribution profiles (Fig. 5A).

Blocks of H3K9me3-labeled heterochromatin appeared in 97% of eight-cell stage IVF nuclei ($n=178$). This labeling was clearly co-localized with CBX1 (Figs 4A and 5A) and in association with CENP dots. It confirms the formation of chromocenters, similar to the somatic ones, at that stage.

When we analyzed NT embryos, we observed that the H3K9me3 distribution of donor cell nuclei was dramatically modified. Twenty hours after the NT, H3K9me3 was distributed as patches in the nuclear volume (Figs 4B and 5B, $n=30$). However, this pattern was not as polarized as in early IVF stages. In comparison to CBX1, no co-localization was observed (Fig. 5B) even for the few nuclei with relatively dense H3K9me3 patches (20%, $n=30$).

Nuclei of two-cell stage NT embryos displayed either patches (64%) or blocks (36%) of H3K9me3 ($n=28$ nuclei or 14 embryos, Fig. 5B). Intriguingly, the patches were polarized within the nuclei like in the two-cell stage IVF embryos (Fig. 4B), whereas the blocks resembled the ones observed in eight-cell IVF embryos with co-localization between CBX1 and H3K9me3 marks, in close proximity to CENP dots. At the four-cell stage, most embryos exhibited nuclei with condensed H3K9me3 blocks (58%, 5 out of 12 embryos, $n=48$ nuclei; Figs 4B and 5B). The nuclei of other embryos (42%) had patches of H3K9me3-labeled heterochromatin distributed on one side of the nuclei and displayed no co-localization with CBX1 similarly to their IVF counterparts (Fig. 5A and B). Finally, the eight-cell stage NT embryos displayed condensed heterochromatin blocks with co-localized CBX1 and H3K9me3 in 95% of the nuclei ($n=130$) similarly to eight-cell stage IVF embryos (Fig. 5A and B).

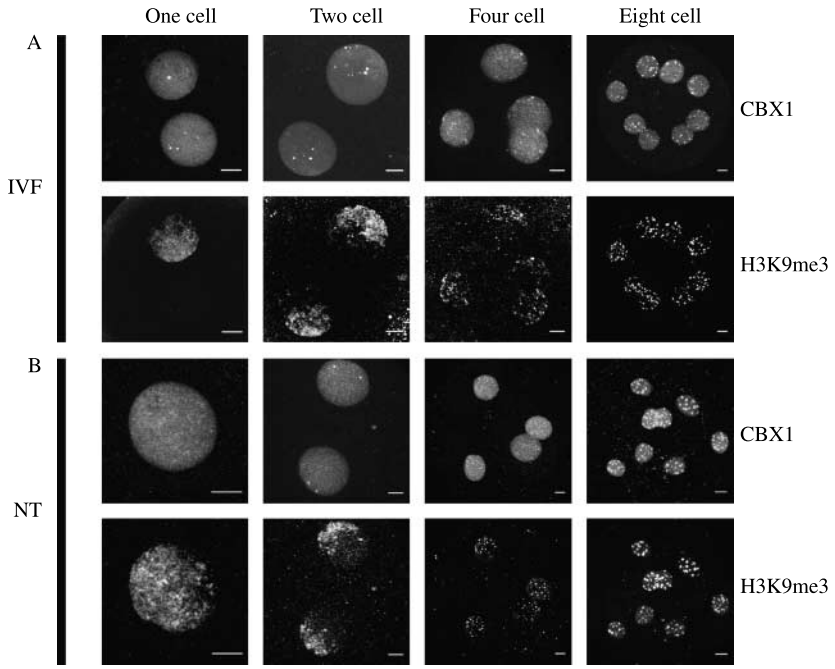

Figure 4 Examples of distribution of heterochromatin simultaneously labeled for CBX1 and H3K9me3 in one- to eight-cell stage IVF (A) and NT (B) embryos. In IVF embryos, CBX1 is similarly distributed in both parental pronuclei at one-cell stage, while H3K9me3 detects polarized patch in female pronuclei only. At two- and four-cell stages, even CBX1 distribution contrasts with labeling of polarized H3K9me3 patches in both types of embryos. Images show condensation of both CBX1 and H3K9me3 patterns at eight-cell stage in IVF embryos and at four- and eight-cell stage in NT embryos. Scale bars: 5 μm.

Discussion

Although a growing number of studies have investigated the functional organization of genomes in nuclei of somatic cells, only a few have addressed remodelling of genome organization during early development, and the impact of NT in species other than mouse. In this study, we investigated the dynamics of genome restructuring in early bovine embryos derived from IVF and from SCNT. We focused on the genesis of chromocenters, i.e. clusters of pericentric heterochromatin regions from several chromosomes, enriched with CBX1 and H3K9me3 marks.

As previously described (Martin *et al.* 2006*a*), we observed a switch of CBX1 distribution in IVF embryos at the eight-cell stage. In this study and the present one, antibodies specific to CENP proteins allowed to discriminate CBX1-labeled chromocenters from other forms of CBX1 distributions. In addition, we demonstrate here that the nuclei of one- to four-cell stage embryos possess noncondensed CBX1 pattern corresponding to spread/fibrous CBX1 distribution (morphological analysis) or small granules (quantitative analysis). As expected, the globular pattern or large granules of CBX1 were found only at eight-cell stage, concurrently with the onset of EGA. We also noticed that all the blastomeres within each embryo from the two- to eight-cell stages exhibited a similar pattern of CBX1 distribution, suggesting a synchronous development. This might indeed be the case as we analyzed embryos in the middle of each embryonic cycle. It should also be pointed out that no spontaneous apoptotic process takes place before EGA, i.e. before the eight-cell stage (Dusan *et al.* 2005). Altogether this could explain the homogeneity we observed among blastomeres in each embryo. Looking at embryos with six-cells or twelve-cells might have given more heterogeneous results.

Our results also show that genome organization of bovine cultured fibroblasts is dramatically modified after NT, since no chromocenters could be observed in one-cell stage NT embryos (as in their IVF counterparts). However, our analysis revealed heterochromatin condensation in some of the embryos from the two-cell stage onwards. Indeed, at the two- and four-cell stages, two types of embryos could be distinguished: one with precocious condensed heterochromatin and another one with noncondensed heterochromatin. These two types of embryos displayed CBX1 and CENP distribution patterns analogous to the ones observed either in eight-cell stage or in two/four-cell stage IVF embryos respectively. This kinetics of heterochromatin restructuring in early NT bovine embryos is schematized in Fig. 6.

EGA in IVF bovine embryos is known to coincide with dramatic changes in nuclear organization (Frei *et al.* 1989, Kanka 2003, Martin *et al.* 2006*a*, 2006*b*). This could also be the case in NT embryos with precociously condensed heterochromatin as major genome activation was previously observed in two- and four-cell stage NT bovine embryos (Smith *et al.* 1996, Lavoir *et al.* 1997). A mechanistic link between these events is provided by the recent discovery of small noncoding RNAs, transcribed from pericentric satellite sequences, which seem to guide proper heterochromatin establishment (Maison & Almouzni 2004, Lu & Gilbert 2007,

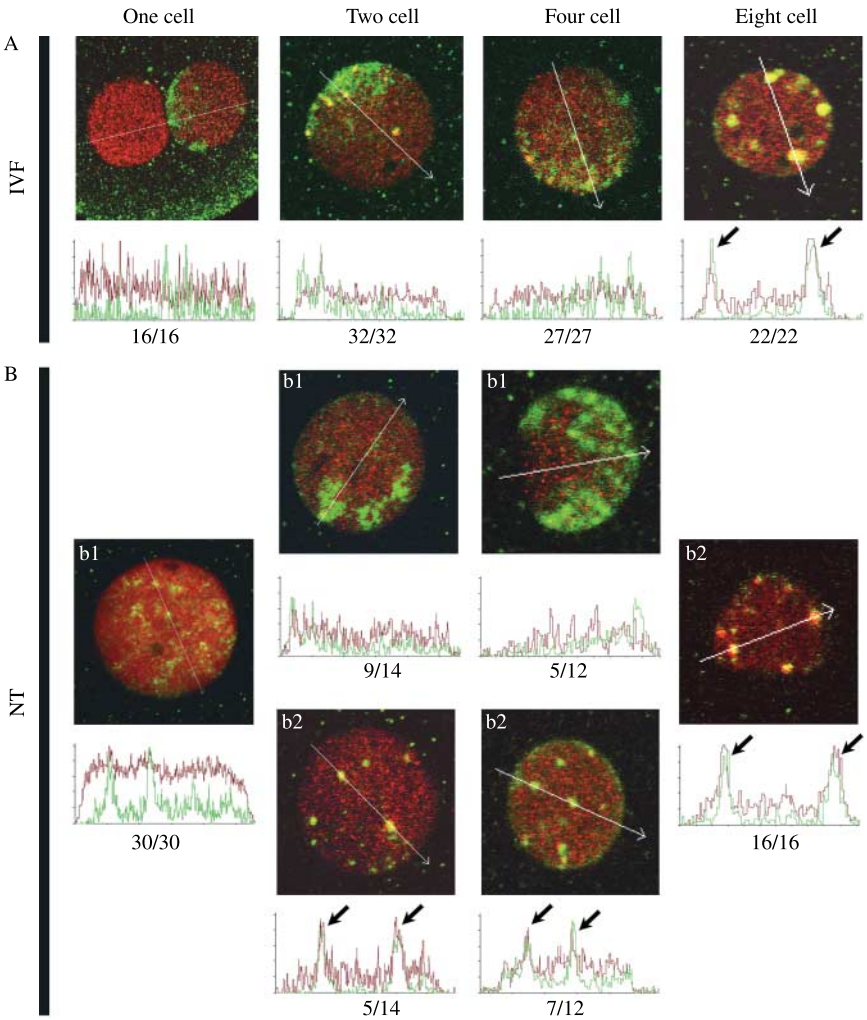

Figure 5 Nuclear distribution of CBX1 (red) and H3K9me3 (green) shown in optical sections in the middle of nuclei of IVF (A) and NT (B) embryos. (A) Dispersed heterochromatin in one-, two-, and four-cell stage IVF embryos is revealed by both marks that do not co-localize; both heterochromatic marks are co-localized upon condensation at eight-cell stage. b1, nucleus from NT embryo with dispersed heterochromatin and H3K9me3 patches; b2, heterochromatin blocks of H3K9me3 co-localized with CBX1 in nuclei of one- to eight-cell stage NT embryos. Numbers below the images show rates of embryos with corresponded type of heterochromatin distribution. Arrows at densitograms indicate co-localization of CBX1 and H3K9me3.

Costa 2008). We therefore hypothesize that, directly or indirectly, transcriptional activation in early embryos is related to chromocenter formation whatever stage they actually appear.

Analysis of H3K9me3 distribution provided another approach to follow constitutive heterochromatin. The distribution of H3K9me3 mark in one-cell cloned embryos was different in comparison with one-cell IVF embryos. Whereas the female pronucleus (the only one to contain this mark) displays a polarized distribution, none of the nuclei in one-cell NT embryos showed evidence of such distribution; instead, H3K9me3-labeled heterochromatin was distributed throughout the nucleus. Since H3K9me3 represents a binding site for CBX1 (Bannister *et al*. 2001, Lachner *et al*. 2001) we expected to find a co-localization of these two marks in nuclei with condensed or noncondensed heterochromatin. Nevertheless, both IVF and NT embryos with noncondensed H3K9me3-labeled heterochromatin displayed mainly uniform nuclear distribution of CBX1, and almost no co-localization of these marks was observed in early developmental stages. This provides evidence that H3K9me3 is not essential for localization of CBX1 to heterochromatin in nuclei with silenced transcription. We therefore believe that this recruitment mechanism is inactive in early bovine embryos with noncondensed heterochromatin and becomes active at later stages either precociously (in part of the NT embryos) or upon the eight-cell stage.

At the molecular level, the establishment of trimethylation at H3K9 in the pericentric chromosomal regions is known to be regulated by histone methyltransferase Suv39h1 (Schotta *et al*. 2002). Moreover, according to Eskeland *et al*. (2007) Suv39h1 facilitates HP1 binding to chromatin methylated at H3K9 and thereby heterochromatin propagation (Stewart *et al*. 2005). In mouse-fertilized embryos, it was already shown that Suv39h is involved in H3K9 methylation of the maternal pronucleus (Puschendorf *et al*. 2008). However, nothing is known in other species, especially concerning NT embryos. On the other hand, the relationship between H3K9 methylation and DNA methylation has been well

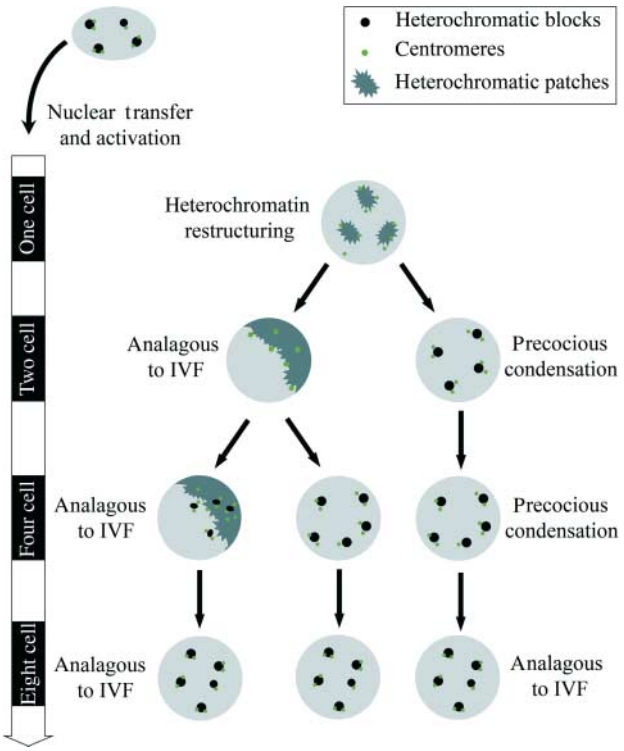

Figure 6 Scheme illustrating two contrasted kinetics of genome restructuring during the four early cell cycles after nuclear transfer in bovine embryos. At one-cell stage, the heterochromatic blocks of donor cell reorganize in patches with irregular distribution of centromeres and spread heterochromatin distribution. At two-cell stage, the heterochromatin is structured as one of two forms: either polarized at nuclear border patches (left) or clusters of condensed heterochromatin (right). At four-cell stage, the number of nuclei with condensed heterochromatin significantly increases. By the eight-cell stage, the chromocenters are formed in a similar proportion as in IVF embryos.

investigated in several species (Santos *et al*. 2003, 2005, Park *et al*. 2007). In cows, a correlation between both marks has been demonstrated in IVF and NT embryos between the two-cell and blastocyst stages (Santos *et al*. 2003). Dean *et al*. (2001) also showed that approximately half of the four-cell NT embryos display precocious increase in DNA methylation level; this roughly corresponds to our estimation of NT embryos with condensed heterochromatin at the same stage. Moreover, Dean *et al*. mentioned the presence of granular structure in the methylated DNA distribution after transcriptional activation in IVF embryos and in four-cell stage NT embryos. This again correlates with our results on H3K9me3-labeled heterochromatin condensation in IVF and NT embryos.

Since restructuring of heterochromatin in early embryonic development is apparently coordinated with the processes of DNA methylation, H3K9 trimethylation, and transcriptional state of the genome, we hypothesize that the two types of nuclear organizations found in NT embryos correspond to contrasted reprograming efficiencies. NT embryos with heterochromatin clusters at the two-cell stage were likely not subjected to any reprograming, and most NT embryos with clusters at the four-cell stage probably had a shortened reprograming period. However, we observed that even in developmentally blocked NT embryos, heterochromatin distribution could be either globular or nonglobular, thus suggesting that CBX1 distribution does not correlate with early developmental failure (data not shown). On the other hand, Santos *et al*. (2003) already demonstrated that H3K9 and DNA methylation reprograming after NT can be related to further developmental potential. We therefore expect early genome restructuring after NT to have long-term effects, for example, through gene expression regulation at the onset of embryonic transcription.

Moreover, since we demonstrated the presence of two types of pericentric heterochromatin distributions in NT embryos, we can predict that these embryos will also display clearly different chromosome territories arrangements. Indeed, changes in high-order chromatin arrangements associated with EGA were shown in IVF bovine embryos (Koehler *et al*. 2009). These authors found that the gene-rich chromosome 19 localizes preferentially at the nuclear periphery before transcriptional activation and shifts towards the nuclear center upon activation at eight-cell stage, whereas the gene-poor chromosome 20 always remains at the nuclear periphery.

Finally, the discovery of two types of heterochromatin distribution dynamics in early development presumes new possibilities to investigate epigenetic and developmental reprograming in NT embryos. Indeed, NT embryos obtained from different donor cell types or after treatment with chemicals such as trichostatin A (Iager *et al*. 2008) could be evaluated for epigenetic reprograming efficiency by investigating their nuclear organization.

Materials and Methods

Maturation of bovine oocytes

The detailed procedure has been previously described (Heyman *et al*. 1994). Ovaries from slaughtered cows were washed in sodium hypochlorite–PBS (0.25%) solution (Sigma) for 5 min, then washed in PBS for 5 min, and kept in sterile PBS at 30–35 °C for transportation to the laboratory (2 h). Cumulus–oocyte complexes were aspirated from 2 to 8 mm diameter follicles and stored in TCM199 (Sigma) at 39 °C. Complexes were rinsed two times in TCM199, then rinsed and matured *in vitro* for 22 h in M199 medium supplemented with 10% FCS (M199–FCS), 10 μg/ml FSH and 10 μg/ml LH (Stimufol, Merial, Lyon, France), and 1 μg/ml estradiol-17β (Sigma), at 39 °C in humidified 5% CO_2 atmosphere.

IVF

After 22 h of maturation, cumulus-expanded oocytes were then inseminated *in vitro* with frozen/thawed bovine sperm. Modified Tyrode's medium was used for capacitation and fertilization according to our standard technique

(Revel *et al*. 1995). After 18–20 h of IVF, cumulus cells were mechanically removed by vortexing and pipetting, and the denuded presumptive zygotes were cultured in microdrops of 50 μl B2 medium (CCD, Paris, France) with 2.5% FCS seeded with Vero cells at 39 °C in humidified 5% CO_2 atmosphere. Embryos at one-cell, two-cell, four-cell, early eight-cell, and late eight-cell stages were fixed with 2% Paraformaldehyde (PFA; Sigma) in PBS for 30 min or overnight after 20, 28, 38, 51, and 69 h post-fertilization respectively.

Nuclear transfer

Matured bovine oocytes were enucleated and processed for NT at 22 h post-maturation as previously described (Gall *et al*. 2008).

Cultured bovine ear fibroblasts at passages 3–10 reaching confluence were used as nuclear donors. Cells were kept at least 48 h at confluence before being collected by trypsinization for NT. Donor cell was introduced by micromanipulation under the zona pellucida of each enucleated oocyte. Cell–oocyte complexes preincubated 1 min in fusion solution (0.3 M mannitol, 0.1 mM $CaCl_2$, and 0.1 mM $MgSO_4$; all from Sigma) were then placed between two electrodes in fusion medium and electrostimulated by two pulses of 2.0 kV/cm for 20 μs to induce the fusion. Reconstructed embryos were incubated for 5 h at 39 °C in humidified 5% CO_2 atmosphere for activation in M199–FCS solution containing 5 μg/ml cytochalasin B and 10 μg/ml cycloheximide (Sigma); fusion efficiency was evaluated 15 min after electrostimulation. After activation, the reconstructed embryos were washed in M199–FCS and B2–FCS solution (5 min each) and cultured in B2 medium like their IVF counterparts. Fixation time points were the same as above.

Immunostaining

After fixation, the embryos were washed for 10 min in PBS and permeabilized by 0.5% Triton X-100/PBS solution (Sigma) for 30 min at room temperature (RT). Embryos were incubated at RT for 1 h in 2% BSA/PBS (BSA from Sigma) to saturate unspecific binding sites. Incubation with the primary antibodies diluted in 2% BSA/PBS was performed for 1 h at 37 °C or overnight at 4 °C in 30 μl antibodies drops under mineral oil. Then the embryos were washed twice (15 min each, RT) in PBS and incubated with the secondary antibodies, diluted in 2% BSA/PBS, for 1 h at RT. Immunostaining controls were performed on fibroblast cells in culture to check that the labeling pattern observed was similar to the one described by the antibody suppliers and by omitting the primary antibodies to avoid any artefact due to unspecific binding of the secondary antibodies. After immunostaining, the embryos were washed for 30 min in PBS at RT and mounted on glass slides with antifading medium (Vectashield, Vector Laboratories, Biovalley, France). Glass coverslips were sealed with nail polish.

CBX1 protein was detected with a specific primary mouse monoclonal anti-HP1β clone 1 MOD 1A9 (Euromedex, Souffelweyersheim, France), diluted 1:200 in 2% BSA/PBS and rhodamine-conjugated anti-mouse secondary antibody (Jackson Immunoresearch, Interchim, France) diluted 1:100 in 2% BSA/PBS. The centromeres were labeled with primary human CREST antibody specific to CENPA and CENPB (Immunovision, Cellon Sarl, Luxembourg), diluted 1:200 in 2% BSA/PBS and FITC-conjugated anti-human secondary antibody (Jackson ImmunoResearch) diluted 1:100 in 2% BSA/PBS. H3K9me3 was detected with primary rat anti-H3K9me3 MAB (Upstate, Millipore, Molsheim, France), diluted 1:200 in 2% BSA/PBS and Cy3-conjugated anti-rat secondary antibody (Jackson ImmunoResearch) diluted 1:100 in 2% BSA/PBS.

Confocal imaging and image analysis

Embryos were observed under a Zeiss LSM 510 confocal microscope (MIMA2 Platform, INRA) using a Plan-Apochromat 63×/1.4 oil objective. Imaging was performed with sequential multitrack scanning using the 488, 543, and 633 nm wavelengths lasers separately. The Z-stacks were acquired using a frame size of 512×512 with a pixel depth of 8 bits and 0.37 μm z-steps.

Automated three-dimensional image processing and analysis were performed with the help of the ITK library (http://www.itk.org) interfaced with Python script language (Lehmann *et al*. 2006). Briefly, images were automatically resized to a constant voxel size (0.284×0.284×0.36 μm). Granules were detected using an automatic threshold segmentation procedure. Therefore, images were processed according to two different methods: the most intense granules were segmented following subtraction of a background image generated by a three-dimensional median filtering, whereas a two-dimensional top-hat filtering was applied to detect small and/or faint granules. The segmented images were then combined and granules parameters were determined. χ^2-test was used to compare nuclei with large granules in NT and IVF embryos at two- and four-cell stages.

Analysis of fluorescence intensity profiles for CBX1 and H3K9me3 was performed with the software LSM510 3.2 version. The optical section in the middle of the Z-stack image was chosen to establish the profiles for both staining along a line drawn across the nuclei. The images for publication were prepared using Adobe Photoshop 8.0.1 version.

Declaration of interest

The authors declare that there is no conflict of interest that could be perceived as prejudicing the impartiality of the research reported.

Funding

This research project was supported by a Marie Curie Early Stage Research Training Fellowship of the European Community's Sixth Framework Programme under contract number MEST-CT-2004-504854.

References

Bannister AJ, Zegerman P, Partridge JF, Miska EA, Thomas JO, Allshire RC & Kouzarides T 2001 Selective recognition of methylated lysine 9 on histone H3 by the HP1 chromo domain. *Nature* **410** 120–124.

Brero A, Easwaran HP, Nowak D, Grunewald I, Cremer T, Leonhardt H & Cardoso MC 2005 Methyl CpG-binding proteins induce large-scale chromatin reorganization during terminal differentiation. *Journal of Cell Biology* **169** 733–743.

Cerda MC, Berrios S, Fernandez-Donoso R, Garagna S & Redi C 1999 Organisation of complex nuclear domains in somatic mouse cells. *Biologie Cellulaire* **91** 55–65.

Cheutin T, McNairn AJ, Jenuwein T, Gilbert DM, Singh PB & Misteli T 2003 Maintenance of stable heterochromatin domains by dynamic HP1 binding. *Science* **299** 721–725.

Costa FF 2008 Non-coding RNAs, epigenetics and complexity. *Gene* **410** 9–17.

Dean W, Santos F, Stojkovic M, Zakhartchenko V, Walter J, Wolf E & Reik W 2001 Conservation of methylation reprogramming in mammalian development: aberrant reprogramming in cloned embryos. *PNAS* **98** 13734–13738.

Dusan F, Koppel J & Maddox-Hyttel P 2005 Apoptotic processes during mammalian preimplantation development. *Theriogenology* **64** 221–231.

Eskeland R, Eberharter A & Imhof A 2007 HP1 binding to chromatin methylated at H3K9 is enhanced by auxiliary factors. *Molecular and Cellular Biology* **27** 453–465.

Frei RE, Schultz GA & Church RB 1989 Qualitative and quantitative changes in protein synthesis occur at the 8–16-cell stage of embryogenesis in the cow. *Journal of Reproduction and Fertility* **86** 637–641.

Fulka H, St John JC, Fulka J & Hozak P 2008 Chromatin in early mammalian embryos: achieving the pluripotent state. *Differentiation* **76** 3–14.

Gall L, Le Bourhis D, Ruffini S, Boulesteix C & Vignon X 2008 Unexpected nuclear localisation of cdc25c in bovine oocytes, early embryos and nuclear-transferred embryos. *Reproduction* **135** 431–438.

Goll MG & Bestor TH 2002 Histone modification and replacement in chromatin activation. *Genes and Development* **16** 1739–1742.

Hayakawa T, Haraguchi T, Masumoto H & Hiraoka Y 2003 Cell cycle behavior of human HP1 subtypes: distinct molecular domains of HP1 are required for their centromeric localization during interphase and metaphase. *Journal of Cell Science* **116** 3327–3338.

Heyman Y, Chesné P, Lebourhis D, Peynot N & Renard JP 1994 Developmental ability of bovine embryos after nuclear transfer based on the nuclear source: *in vivo* versus *in vitro*. *Theriogenology* **42** 695–702.

Iager AE, Ragina NP, Ross PJ, Beyhan Z, Cunniff K, Rodriguez RM & Cibelli JB 2008 Trichostatin A improves histone acetylation in bovine somatic cell nuclear transfer early embryos. *Cloning and Stem Cells* **10** 371–379.

Kanka J 2003 Gene expression and chromatin structure in the preimplantation embryo. *Theriogenology* **59** 3–19.

Koehler D, Zakhartchenko V, Froenicke L, Stone G, Stanyon R, Wolf E, Cremer T& & Brero A 2009 Changes of higher order chromatin arrangements during major genome activation in bovine preimplantation embryos. *Experimental Cell Research* **315** 2053–2063.

Lachner M, O'Carroll D, Rea S, Mechtler K & Jenuwein T 2001 Methylation of histone H3 lysine 9 creates a binding site for HP1 proteins. *Nature* **410** 116–120.

Lachner M, O'Sullivan RJ & Jenuwein T 2003 An epigenetic road map for histone lysine methylation. *Journal of Cell Science* **116** 2117–2124.

Latham KE 1999 Mechanisms and control of embryonic genome activation in mammalian embryos. *International Review of Cytology* **193** 71–124.

Lavoir MC, Kelk D, Rumph N, Barnes F, Betteridge KJ & King WA 1997 Transcription and translation in bovine nuclear transfer embryos. *Biology of Reproduction* **57** 204–213.

Lehmann G, Pincus Z & Regrain B 2006 Wrap ITK: Enhanced languages support for the Insight Toolkit. *The Insight Journal* http://hdl.handle.net/1926/188.

Loi P, Beaujean N, Khochbin S, Fulka J Jr & Ptak G 2008 Asymmetric nuclear reprogramming in somatic cell nuclear transfer? *BioEssays* **30** 66–74.

Lu J & Gilbert DM 2007 Proliferation-dependent and cell cycle regulated transcription of mouse pericentric heterochromatin. *Journal of Cell Biology* **179** 411–421.

Maddox-Hyttel P, Bjerregaard B & Laurincik J 2005 Meiosis and embryo technology: renaissance of the nucleolus. *Reproduction, Fertility, and Development* **17** 3–14.

Maison C & Almouzni G 2004 HP1 and the dynamics of heterochromatin maintenance. *Nature Reviews. Molecular Cell Biology* **5** 296–304.

Martin C, Beaujean N, Brochard V, Audouard C, Zink D & Debey P 2006*a* Genome restructuring in mouse embryos during reprogramming and early development. *Developmental Biology* **292** 317–332.

Martin C, Brochard V, Migne C, Zink D, Debey P & Beaujean N 2006*b* Architectural reorganization of the nuclei upon transfer into oocytes accompanies genome reprogramming. *Molecular Reproduction and Development* **73** 1102–1111.

Mayer W, Niveleau A, Walter J, Fundele R & Haaf T 2000 Demethylation of the zygotic paternal genome. *Nature* **403** 501–502.

Mayer R, Brero A, von Hase J, Schroeder T, Cremer T & Dietzel S 2005 Common themes and cell type specific variations of higher order chromatin arrangements in the mouse. *BMC Cell Biology* **6** 44.

Merico V, Barbieri J, Zuccotti M, Joffe B, Cremer T, Redi CA, Solovei I & Garagna S 2007 Epigenomic differentiation in mouse preimplantation nuclei of biparental, parthenote and cloned embryos. *Chromosome Research* **15** 341–360.

Park JS, Jeong YS, Shin ST, Lee KK & Kang YK 2007 Dynamic DNA methylation reprogramming: active demethylation and immediate remethylation in the male pronucleus of bovine zygotes. *Developmental Dynamics* **236** 2523–2533.

Probst AV, Santos F, Reik W, Almouzni G & Dean W 2007 Structural differences in centromeric heterochromatin are spatially reconciled on fertilisation in the mouse zygote. *Chromosoma* **116** 403–415.

Prusov AN & Zatsepina OV 2002 Isolation of the chromocenter fraction from mouse liver nuclei. *Biochemistry* **67** 423–431.

Puschendorf M, Terranova R, Boutsma E, Mao X, Isono K, Brykczynska U, Kolb C, Otte AP, Koseki H, Orkin SH *et al.* 2008 PRC1 and Suv39h specify parental asymmetry at constitutive heterochromatin in early mouse embryos. *Nature Genetics* **40** 411–420.

Revel F, Mermillod P, Peynot N, Renard JP & Heyman Y 1995 Low developmental capacity of *in vitro* matured and fertilized oocytes from calves compared with that of the cows. *Journal of Reproduction and Fertility* **103** 115–120.

Santos F, Hendrich B, Reik W & Dean W 2002 Dynamic reprogramming of DNA methylation in the early mouse embryo. *Developmental Biology* **241** 172–182.

Santos F, Zakhartchenko V, Stojkovic M, Peters A, Jenuwein T, Wolf E, Reik W & Dean W 2003 Epigenetic marking correlates with developmental potential in cloned bovine preimplantation embryos. *Current Biology* **13** 1116–1121.

Santos F, Peters AH, Otte AP, Reik W & Dean W 2005 Dynamic chromatin modifications characterise the first cell cycle in mouse embryos. *Developmental Biology* **280** 225–236.

Schneider R & Grosschedl R 2007 Dynamics and interplay of nuclear architecture, genome organization, and gene expression. *Genes and Development* **21** 3027–3043.

Schotta G, Ebert A, Krauss V, Fischer A, Hoffmann J, Rea S, Jenuwein T, Dorn R & Reuter G 2002 Central role of *drosophila* SU(VAR)3–9 in histone H3-K9 methylation and heterochromatic gene silencing. *EMBO Journal* **21** 1121–1131.

Smith SD, Soloy E, Kanka J, Holm P & Callesen H 1996 Influence of recipient cytoplasm cell stage on transcription in bovine nucleus transfer embryos. *Molecular Reproduction and Development* **45** 444–450.

Solovei I, Schermelleh L, During K, Engelhardt A, Stein S, Cremer C & Cremer T 2004 Differences in centromere positioning of cycling and postmitotic human cell types. *Chromosoma* **112** 410–423.

Stewart MD, Li J & Wong J 2005 Relationship between histone H3 lysine 9 methylation, transcription repression, and heterochromatin protein 1 recruitment. *Molecular and Cellular Biology* **25** 2525–2538.

Wiblin AE, Cui W, Clark AJ & Bickmore WA 2005 Distinctive nuclear organisation of centromeres and regions involved in pluripotency in human embryonic stem cells. *Journal of Cell Science* **118** 3861–3868.

Received 16 October 2008
First decision 4 December 2008
Revised manuscript received 19 September 2009
Accepted 24 September 2009